Characterization by Fluorescence of the Distribution of Maleic Anhydride Grafted onto Ethylene−Propylene Copolymers

Mingzhen Zhang and Jean Duhamel*

Institute for Polymer Research, Department of Chemistry, University of Waterloo, Waterloo, Ontario N2L 3G1, Canada

Martin van Duin and Patric Meessen

DSM Research, P.O. Box 18, 6160 MD Geleen, The Netherlands

Received December 15, 2003; Revised Manuscript Received December 17, 2003

ABSTRACT: An ethylene−propylene random copolymer (EP) was maleated according to two different procedures which were expected to yield different distributions of succinic anhydride (SAH) along the backbone. The two maleated EPs, referred to as EP-I and EP-II, were labeled with fluorescent dyes such as pyrene and/or naphthalene by reacting 1-pyrenemethylamine (or 1-naphthalenemethylamine) with the SAH moieties randomly attached along the EP copolymer. As a result, the distribution of dyes mimics that of the SAH moieties along the polymer backbone. The labeled EP copolymers thus obtained were studied by steady-state and time-resolved fluorescence techniques in solution. Hexane and tetrahydrofuran (THF) were chosen as solvents. Pyrene excimer formation and fluorescence resonance energy transfer measurements were performed to demonstrate that the SAH moieties are attached to EP-I in a less clustered manner than to EP-II. These conclusions were confirmed by analyzing the fluorescence decays of the pyrene-labeled EPs with a blob model developed in the laboratory. Viscosity measurements were performed on both pyrene-labeled EP copolymers to evaluate the effect that SAH clustering has on the solution properties of the polymers in hexane. The solution viscosity of the pyrene-labeled EP-I increases less steeply with polymer concentration than that of the pyrene-labeled EP-II. This effect is due to the higher SAH clustering observed with EP-II, which leads to a more efficient formation of interpolymeric aggregates held together via dipolar associations between the anhydride moieties. This study establishes that fluorescence can be applied to investigate the microstructure of maleated EP copolymers and that SAH clustering of a maleated EP copolymer can affect its properties in apolar solvents.

Introduction

Polyolefins are generally nonreactive polymers. However they can be functionalized by attaching reactive groups onto their backbone.[1−4] In this respect, the grafting of polyolefins with maleic anhydride (MAH) has received much attention owing to their large number of applications.[5] For instance, polyamides can be mixed with ethylene−propylene random copolymers (EP) grafted with MAH (EP-MAH) in a heterogeneous melt to react with the succinic anhydride (SAH) moieties of the modified polyolefin. This process generates imide linkages between the two polymers and results in improved dispersion and adhesion between the two incompatible polymers. The use of EP-MAHs as compatibilizing agents in blends[6] have led to the production of super-tough polyamides.[7]

EP-MAH can also be reacted with amines yielding succinimide groups again. These modified polyolefins are used as additives for motor oils, where they can act as viscosity modifiers and particle stabilizers.[8] During the normal operation of an engine, polar particulate matter is being generated in the oil. The polar succinimide groups associate with the polar surface of the colloidal particles, which are stabilized by the oil-soluble polyolefin backbone.

MAH grafting can be achieved using melt[9] or solution routes.[10] Typically the polyolefin is mixed with MAH and an initiator such as a suitable peroxide.[11] This procedure yields a polyolefin randomly grafted with MAH. Modification with MAH at specific positions of a polyolefin has also been reported. Using an Alder-Ene reaction[12g] or a dehydrochlorination reaction,[12b] MAH can be attached specifically at the unsaturated ends of an oligoisobutylene. These modified oligoisobutylenes are used as colloid stabilizers in motor oils.[8]

Although the synthetic procedures for achieving MAH grafting are usually straightforward, there is still debate on the nature of the grafted product. Acid−base titration, IR spectroscopy and ^{1}H and ^{13}C NMR provide information about the level of grafting. Information about the nature of the grafts has been obtained mostly by ^{13}C NMR[13,14] and to a much lesser extent by IR spectroscopy.[9j] However, many such studies often lead to contradictory conclusions. In 1996, Heinen et al. carried out a thorough ^{13}C NMR study of the grafting of ^{13}C-enriched MAH onto polyethylene, polypropylene, and EP copolymers with different ethylene contents. Their work unambiguously established that (1) MAH attaches to the high density and low-density polyethylene in the form of single succinic anhydride units as well as very short oligomers and (2) MAH forms single succinic anhydride units when grafted onto polypropylene or ethylene−propylene random copolymers with abundant propylene content.

Although the nature of the MAH grafts was clearly established by the ^{13}C NMR study carried out by Heinen et al.,[13] these measurements do not allow the characterization of commercial MAH-grafted polyolefins because ^{13}C NMR is not very sensitive for non-^{13}C-labeled MAH pendants and the low levels of MAH grafting used in typical EP-MAH (<2 wt %) usually preclude a

* To whom correspondence should be addressed.

10.1021/ma035906e CCC: $27.50
Published on Web 02/05/2004

Scheme 1

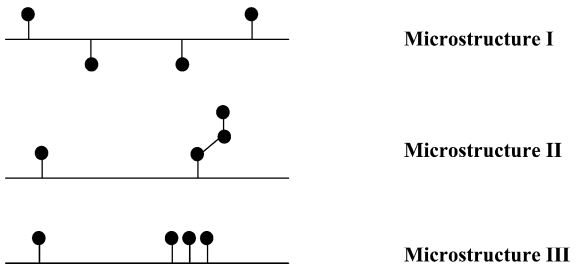

detailed analysis of the grafted polyolefin. The grafting of single saturated SAH is usually reported (cf. Scheme 1, microstructure **I**).[9g,12b,13,15] However, it has also been shown that oligomeric or polymeric MAH grafts can be formed (cf. Scheme 1, microstructure **II**).[9a,9h−j,13,14] More recently, microstructure **III** in Scheme 1 has been proposed, where MAH is attached to the backbone as both individual and clustered units.[16]

Since the blend compatibilizing, oil dispersion, and rheological properties of EP-MAH can be expected to depend on the grafts microstructure, a detailed knowledge of the nature of the grafted units (whether isolated SAH units, oligoSAH, or clustered SAH) is important for improving EP-MAH properties. Considering the microstructures displayed in Scheme 1, there is no doubt that a technique capable of distinguishing between clustered (or oligomerized) SAH and less clustered SAH (or isolated) units would be a valuable tool for the characterization of EP-MAH microstructure. In this article, the microstructure of an EP-MAH refers to the distribution of the SAH units along the EP backbone.

To this date, the level of SAH clustering of a maleated EP copolymer can only be inferred from its rheological behavior. In an apolar solvent, the polar SAH groups induce the formation of an interpolymeric network held together by polar aggregates of the SAH pendants. Interpolymeric associations of hydrophobically modified water-soluble polymers have been shown to be more efficient in water when the associative pendants are distributed in a clustered manner.[17] Consequently, the viscosity of a polymer solution is expected to increase more quickly with polymer concentration when the associating moieties are clustered along the chain. To determine the level of SAH clustering of a maleated EP copolymer, a researcher must compare the viscosity-vs-concentration profile of the modified polymer with that of others used as standards. However, even this simple experiment is difficult to carry out due to the absence of maleated EP standards resulting from the poor level of characterization of the structures obtained by MAH grafting, as illustrated by the contradictory conclusions drawn by different research groups (cf. Scheme 1).[9,12−16] Furthermore, the assignment of the level of SAH clustering of a maleated EP copolymer via viscosity measurements is an indirect measurement. The characterization of maleated EP copolymers would be greatly improved if the level of SAH clustering could be measured in a direct manner.

Earlier works from this laboratory have shown that fluorescence experiments have the potential to yield the level of SAH clustering of EP-MAHs.[18] These experiments require attaching the dye pyrene onto the SAH moieties of an EP-MAH. Upon absorption of a photon, the encounter of an excited pyrene with a ground-state pyrene leads to the formation of an excited complex called an excimer. The time scale of excimer formation depends on whether the two pyrenes are attached onto SAH moieties which are clustered or isolated. Careful analysis of the fluorescence decays of the pyrene monomer and excimer can distinguish between the two time scales and provide a direct measurement of the level of SAH clustering. However, our earlier attempts were cumbersome, and the results about the level of SAH clustering could not be validated for the following reasons.

The early experiments performed by this laboratory to determine the level of SAH clustering involved the labeling of the SAH pendants of an EP-MAH with 1-pyrenebutanoic acid hydrazide.[18] These studies were very complicated due to the five-atom linker connecting the SAH moiety to the pyrene chromophore (cf. Scheme 2). The complications arose from the decoupling taking place between the slow motions of the polymer backbone and the rapid ones of the pyrene moiety enabled by the flexible linker. An additional rate constant was needed to properly handle the fluorescence decays. Accounting for the additional rate constant led to rather cumbersome equations, particularly for the study of the pyrene labeled EP copolymer in hexane.[18] To avoid these complications, we reasoned that using 1-pyrenemethylamine instead of 1-pyrenebutanoic acid hydrazide would strongly reduce the freedom of motion of the pyrene moiety with respect to the EP backbone (cf. Scheme 2) as had been suggested in an earlier work.[19] The complications were indeed eliminated, and all the decays presented in the present work could be satisfyingly fitted with the simple and now well-established blob model equation.[20−23]

Since we improved the design of the labeled EP copolymer and simplified the analysis procedure, it became essential to test it with a set of EP-MAHs exhibiting different levels of SAH clustering. Unfortunately such samples are very difficult to come by. Since the level of SAH clustering can only be inferred from viscosity measurements, the EP-MAH samples must have the same molecular weights, molecular weight distributions, and the same level of MAH grafting, because all these parameters affect viscosity measurements. DSM provided us with two maleated EP copolymers exhibiting the required features. The EP-MAHs were labeled with 1-pyrenemethylamine and 1-naphthalenemethylamine. Fluorescence resonance energy transfer (FRET) and fluorescence blob model experiments were carried out to characterize their MAH microstructure qualitatively and quantitatively, respectively. The thorough characterization of the MAH microstructure was then used to rationalize the viscosity-vs-concentration profiles of solutions of the two pyrene-labeled EP-MAHs in hexane. To the best of our knowledge, the fluorescence experiments presented in this manuscript represent the only means available today to obtain directly a quantitative measure of the level of SAH clustering of an EP-MAH.

Experimental Section

Materials. Anhydrous dodecane, naphthalene, 1-pyrenemethylamine, and 1-naphthalenemethylamine were purchased from Sigma-Aldrich. Solvents of spectrograde quality (acetone and hexane) were purchased from EM Science. THF (distilled in glass) was purchased from Caledon. All solvents were used as received unless otherwise specified. The two maleated EP copolymers, EP-I and EP-II, were provided by DSM (The Netherlands). All molecular weights of EP copolymers were determined by gel permeation chromatography (GPC) in

Scheme 2

Labeling of an EP-MAH with 1-pyrenebutanoic acid hydrazide

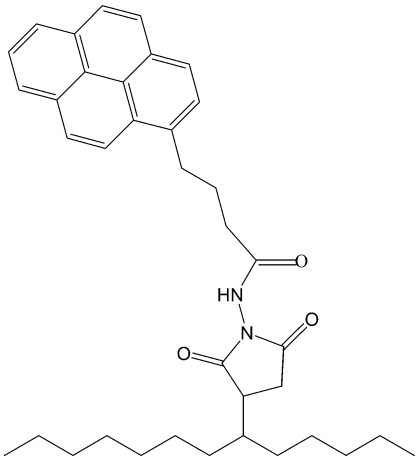

Labeling of an EP-MAH with 1-pyrenemethylamine

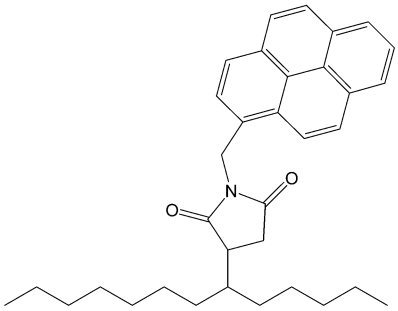

Table 1. Apparent Molecular Weight, Ethylene Content, and Level of MAH Grafting of EP-MAHs[a]

polymers	M_n (kg/mol)	M_w/M_n	ethylene (wt %)	MAH grafted (μmol/g of polymer)	no. of MAH grafts per chain
EP-I	28	2.8	49	151	4.2
EP-II	28	2.8	49	147	4.1

[a] Data provided by DSM.

trichlorobenzene using universal calibration.[24] The ethylene content and the level of MAH grafting of EP-I and EP-II were determined by DSM using FTIR spectroscopy and are summarized in Table 1. EP-III, a nonmaleated EP copolymer, was supplied by Imperial Oil.

Determination of the Level of Maleic Anhydride. The level of MAH grafting for EP-I and EP-II was measured via solution FT-IR using a calibration curve. The calibration curve was obtained from five samples whose MAH concentrations were determined by solution ^{1}H NMR.

Gel Permeation Chromatography. A Waters 150C high-temperature GPC equipped with a Viscotek viscometer and the recommended operating conditions of ASTM Standard D 6474[25] were used. The suggested ASTM Standard D 6474 operating conditions include a column temperature of 140 °C, 1,2,4-trichlorobenzene with added antioxidant as a solvent, a flow rate of 1.0 mL/min, a sample concentration of 0.1 wt %, and commercially available polystyrene standards for calibration.

Pyrene Labeling. Maleated EP copolymer (0.3 g) was introduced in a 100 mL round flask to which 15 mL anhydrous dodecane was added. The flask was subject to three freeze−thaw cycles before it was heated to 130 °C under nitrogen for 6 h. This ensured that all SAH which might have hydrolyzed over time to the corresponding acid reverted to the cyclized form. Then 15 mL of a 1-pyrenemethylamine (PMA) solution in hexane ([PMA] = 4.1×10^{-3} M) was added. An excess of 20−25% PMA was fed to the reaction vessel to ensure that all the MAH pendants reacted to completion. Hexane was then removed. The mixture was stirred and the reaction allowed to proceed for 18 h at 180 °C under nitrogen. The polymer was precipitated from dodecane into acetone. The resulting polymer was purified by precipitation from hexane into acetone. The precipitation was repeated for at least five times until the polymer was completely free of unreacted PMA. A list of the pyrene labeled copolymers prepared in duplicate (reactions R1 and R2) is given in Table 2. The reactions were duplicated to estimate the reproducibility of the experiments. The pyrene content of all polymers equaled 160±10 μmol of pyrene per gram of polymer. The number-average molecular weights of Py-EP-I-R2 and Py-EP-II-R2 were determined to equal 41 ± 1 kg/mol by GPC (cf. Table 7). It appears that the shorter chains of the original polymers (M_n = 28 kg/mol, cf. Table 1) were fractionated out during the repeated cycles of precipitation.

Table 2. UV/Vis Characterization of Py-Labeled EP-MAHs

Py-labeled EP-MAHs	Py content λ (μmol/g of polymer)	no. of ethylene and propylene units per Py	mol % labeling	P_A (THF)	P_A (hexane)
Py-EP-I-R1	170	174	0.57	3.1	1.8
Py-EP-I-R2	166	179	0.56	3.2	1.9
Py-EP-II-R1	150	198	0.51	2.7	1.9
Py-EP-II-R2	163	182	0.55	2.8	1.9

Table 3. Steady-State Fluorescence Properties of Py-EPs

	λ (μmol/g of polymer)	solvent	I_E/I_M at 344 nm excitation
Py-EP-I-R1	170	THF	0.56
Py-EP-I-R2	166		0.64
Py-EP-II-R1	150		0.72
Py-EP-II-R2	163		0.74
Py-EP-I-R1	170	hexane	1.77
Py-EP-I-R2	166		1.75
Py-EP-II-R1	150		1.92
Py-EP-II-R2	163		1.96

Doubly Labeled Copolymers and Naphthalene Labeling. These polymers were prepared by following the same procedure used for the pyrene-labeled EP copolymers. The only difference in procedure was the addition of solutions of 1-naphthalenemethylamine (NMA) and PMA in hexane to the reaction flask. A list of the doubly labeled EP copolymers is given in Table 5. The average dye content equals 140 ± 20 μmol/g and is close to those obtained for the pyrene-labeled EP copolymers, although it is a little lower and more scattered. For the doubly labeled EP copolymers, the fraction of the dyes which are pyrene ranges from 0 to 43 mol %.

Fourier Transform Infrared (FT-IR) spectroscopy. FT-IR spectra were recorded on a MB-series Bomem spectrophotometer. The presence of MAH attached onto the polymer could be detected by monitoring the absorption peak at 1788 cm^{-1} characteristic of the anhydride carbonyl. After EP-MAH had reacted with PMA or NMA, the peak at 1788 cm^{-1} disappeared and a new peak appeared at 1710 cm^{-1} characteristic of the presence of succinimide carbonyls (cf. Figure 1).

UV−Vis Absorption Measurements. Absorption spectra were carried out on a Hewlett-Packard 8452A diode array spectrophotometer.

Table 4. Parameters Obtained from the Fit of the Fluorescence Decays of the Py-EPs with a Sum of Exponentials

A. Monomer: Four Exponentials

sample	λ (μmol/g of polymer)	solvent	τ_{m1} (ns)	a_{m1}	τ_{m2} (ns)	a_{m2}	τ_{m3} (ns)	a_{m3}	τ_{m4} (ns)	a_{m4}	χ^2
Py-EP-I-R1	170	THF	8	0.42	43	0.29	147	0.21	290	0.08	0.89
Py-EP-I-R2	166		11	0.36	51	0.32	145	0.23	290	0.10	1.01
Py-EP-II-R1	150		16	0.35	60	0.36	181	0.24	290	0.05	1.07
Py-EP-II-R2	163		18	0.43	70	0.30	181	0.20	290	0.07	1.03
Py-EP-I-R1	170	hexane	11	0.31	54	0.31	159	0.24	350	0.14	0.99
Py-EP-I-R2	166		10	0.33	44	0.28	140	0.23	350	0.15	1.08
Py-EP-II-R1	150		17	0.41	64	0.30	178	0.28	350	0.01	1.13
Py-EP-II-R2	163		23	0.40	101	0.36	284	0.23	350	0.01	0.96

B. Excimer: Three Exponentials

sample	λ (μmol/g of polymer)	solvent	τ_{e1} (ns)	$a_{e1}/(a_{e2}+a_{e3})$	τ_{e2} (ns)	$a_{e2}/(a_{e2}+a_{e3})$	τ_{e3} (ns)	$a_{e3}/(a_{e2}+a_{e3})$	χ^2
Py-EP-I-R1	170	THF	16	−0.62	75	0.90	156	0.10	1.10
Py-EP-I-R2	166		24	−0.59	71	0.90	162	0.10	1.02
Py-EP-II-R1	150		17	−0.41	69	0.89	141	0.11	1.13
Py-EP-II-R2	163		18	−0.38	70	0.93	171	0.07	1.02
Py-EP-I-R1	170	hexane	17	−0.28	68	0.90	157	0.10	1.15
Py-EP-I-R2	166		16	−0.28	66	0.91	149	0.09	1.05
Py-EP-II-R1	150		38	−0.02	63	0.95	146	0.05	1.01
Py-EP-II-R2[a]	163				63	0.85	129	0.15	1.00

[a] No rise time could be detected in the excimer decay.

Table 5. FRET Data of Doubly Labeled EP-MAHs

sample	solvent	overall dye content (μmol/g of polymer)	Py mol %	I_{375}/I_{323}
Py40-Np60-EP-I	THF	116	40	5.9
Py20-Np80-EP-I		161	20	1.9
Py9-Np91-EP-I		151	9	0.6
Np-EP-I		145	0	0.2
Py43-Np57-EP-II	THF	118	43	21
Py24-Np76-EP-II		148	24	5.4
Py11-Np89-EP-II		152	11	2.0
Np-EP-II		121	0	0.2
Py40-Np60-EP-I	hexane	116	40	9.4
Py20-Np80-EP-I		161	20	3.2
Py9-Np91-EP-I		151	9	1.2
Np-EP-I		145	0	0.4
Py43-Np57-EP-II	hexane	118	43	91.0
Py24-Np76-EP-II		148	24	33.1
Py11-Np89-EP-II		152	11	7.7
Np-EP-II		121	0	0.5

Pyrene (Py) Content of the Py-Labeled Copolymer. The Py content of the polymer was established by measuring the absorption of a solution prepared from a carefully weighed amount, m, of Py-labeled polymer in a known volume, V, of THF. The Py concentration, [Py], was then estimated from the absorption value at 344 nm and the extinction coefficient of a Py model compound, typically 1-pyrenemethanol (ϵ [344 nm, in THF] = 42 700 cm^{-1} M^{-1}). The Py content, λ, of the polymer could be calculated from $\lambda = [Py]V/m$ expressed in moles of Py per gram of polymer.

Naphthalene (Np) Content of the Np-Labeled Copolymer. A similar procedure was applied to determine the Np content of the Np-labeled polymers using the extinction coefficient of NMA at 282 nm (ϵ [for NMA at 282 nm, in THF] = 6700 cm^{-1} M^{-1}).

Naphthalene and Pyrene Contents of the Doubly Labeled Copolymers. First, the Py content of the doubly labeled copolymers was determined following the procedure described above. The absorption resulting from Np was determined by recording the absorption spectrum of the doubly labeled polymer and subtracting from it the absorption spectrum of a Py-labeled copolymer normalized at 344 nm. The extinction coefficient of a Np model compound, typically NMA was used to determine the Np concentration [Np]. It was then employed to determine the Np content, λ, expressed in moles of Np per gram of polymer, using the relationship, $\lambda = [Np]V/m$, where V and m have been defined in the previous section.

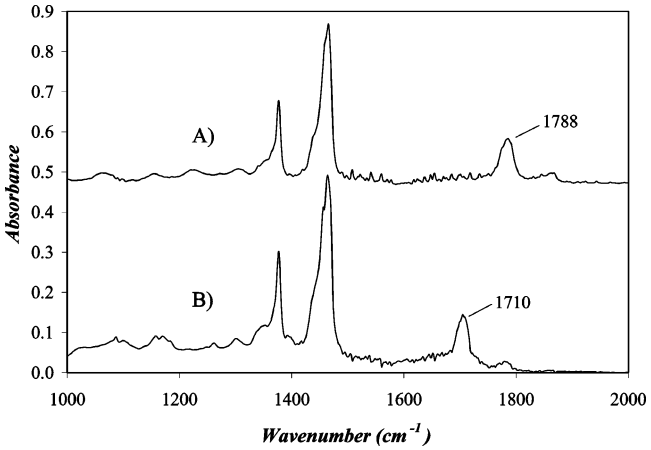

Figure 1. Infrared spectra of (A) EP-MAH and (B) pyrene-labeled EP-MAH

Sample Preparation for Fluorescence Measurements. All the polymer solutions for fluorescence measurements were degassed under a gentle flow of nitrogen for 20 min and had dye concentrations around 2.5×10^{-6} M and 1.8×10^{-5} M for the Py-labeled and Np-labeled copolymers, respectively. These dye concentrations ensured that the absorption at the excitation wavelength for the fluorescence experiments (290 and 344 nm for Np and Py, respectively) was no larger than 0.1 to avoid artifacts due to the inner filter effect.[26a] These concentrations were sufficiently small so that no intermolecular interactions took place, as will be established later.

Steady-State Fluorescence Spectroscopy. Steady-state fluorescence spectra were recorded on a Photon Technology International LS-100 steady-state system with a pulsed xenon flash lamp as the light source. The slit widths on the excitation and emission monochromators equaled 2 and 1 nm, respectively. All spectra were obtained with a right-angle configuration. The Py-labeled polymer samples were excited at 344 nm. The fluorescence intensities of the monomer (I_M) and of the excimer (I_E) were calculated by taking the integrals under the fluorescence spectra from 372 to 378 nm for the Py monomer, and from 500 to 530 nm for the Py excimer. The excimer fluorescence intensity is considered for wavelengths

above 500 nm to avoid potential overlap with the Py monomer fluorescence. The Np-labeled copolymers were excited at 290 nm. The fluorescence intensity of Np (I_{Np}) was calculated by taking the integral under the fluorescence spectra from 320 to 326 nm.

Time-Resolved Fluorescence Spectroscopy. Decay curves were obtained by the time-correlated single-photon counting (TCSPC) technique. These were measured by a Photochemical Research Associates (PRA), Inc., System 2000. For Py-labeled copolymers, the excitation wavelength was 344 nm, and the fluorescence from the Py monomer and excimer was monitored at 375 and 510 nm, respectively. To block potential light scattering leaking through the detection system, filters were used with a cutoff at 370 and 495 nm to acquire the fluorescence decays of the Py monomer and excimer, respectively. All decays were collected over 512 channels. A total of 20 000 counts was collected at the peak maximum of the lamp and the decay curves. The analyses of the decay curves were performed with the δ-pulse deconvolution. Reference decay curves of degassed solutions of PPO [2,5-diphenyloxazole] in cyclohexane (τ = 1.42 ns) and BBOT [2,5-bis(5-*tert*-butyl-2-benzoxazolyl) thiophene] in ethanol (τ = 1.47 ns) were used for the analyses of the monomer and excimer decay curves, respectively. A similar procedure was employed to acquire the Np monomer decays for the Np-labeled copolymers. Solutions were excited at 290 nm and the fluorescence from the Np monomer was monitored at 338 nm. To block potential light scattering leaking through the detection system, a filter was used with a cutoff at 335 nm.

Analysis of the Fluorescence Decays. As in other studies, the assumed function $g(t)$ for the fluorescence decays was convoluted with the instrument response function to fit the experimental decay.[18,20−23] A light-scattering correction was applied to the fluorescence analysis to account for residual light scattering reaching the detector, as well as for those dyes attached close to one another which either form an excimer or undergo energy transfer on a subnanosecond time scale, too short to be detected by our time-resolved fluorometer.[27] Several $g(t)$ functions were used. First the decays were fitted with a sum of exponentials with an expression given in eq 1 where the number of exponentials n is varied from 1 to 4. The index X in eq 1 is either M or E for the monomer or the excimer, respectively. The parameters of $g(t)$ were retrieved by using a least-squares curve fitting program based on the Marquardt−Levenberg algorithm.[28]

$$g(t) = \sum_{\substack{i=1 \\ X=M,E}}^{i=n} A_{Xi} e^{-t/\tau_{Xi}} \quad (1)$$

The monomer fluorescence decays were also fitted by the function $g(t)$ given by eq 2 which handles the kinetics of encounter between pyrenes attached onto EP copolymers according to the *blob* model. The derivation of eq 2 was carried out in an earlier paper[20] using Tachiya's mathematical treatment.[29]

$$[Py^*]_{(t)} = f \exp\left[-\left(A_2 + \frac{1}{\tau_M}\right)t - A_3(1 - \exp(-A_4 t))\right] + (1 - f)\exp(-t/\tau_M) \quad (2)$$

The parameters A_2, A_3, and A_4 are described in eq 3.

$$A_2 = \langle n \rangle \frac{k_{blob} k_e [blob]}{k_{blob} + k_e [blob]} \quad A_3 = \langle n \rangle \frac{{k_{blob}}^2}{(k_{blob} + k_e [blob])^2} \quad A_4 = k_{blob} + k_e [blob] \quad (3)$$

These equations are very similar to those obtained for pyrene excimer formation in micellar systems.[30]

The time-dependent behavior of the excited pyrene monomers given by eq 2 uses the parameter f, which refers to the fraction of pyrene monomers that form excimer by diffusion. The fraction $(1 - f)$ refers to the pyrenes that do not form excimer and fluoresce with their natural lifetime τ_M. The parameters $\langle n \rangle$, k_{blob}, and $k_e[blob]$ refer to the average number of pyrene groups per *blob*, the rate constant of excimer formation inside a *blob* containing one excited pyrene and one ground-state pyrene only, and the rate at which pyrene groups exchange between *blobs*, respectively. Here, k_e is the exchange rate constant and [*blob*] is the *blob* concentration inside the polymer coil. The Marquardt−Levenberg algorithm is applied to retrieve the parameters A_2, A_3, and A_4 from the fit of the fluorescence decays. The excimer fluorescence decays were fitted with eq 4 and optimized as discussed in earlier publications.[21−23] For all fluorescence decays, the fit was considered good if the χ^2 parameter was less than 1.30 and if the residuals and the autocorrelation function of the residuals were randomly distributed around zero.

$$[E^*] = -[Py^*_{diff}]_{(t=0)} e^{-A_3} \sum_{i=0}^{\infty} \frac{{A_3}^i}{i!} \frac{A_2 + iA_4}{\frac{1}{\tau_M} - \frac{1}{\tau_{E0}} + A_2 + iA_4} \times \exp\left(-\left(\frac{1}{\tau_M} + A_2 + iA_4\right)t\right) + \left([E0^*]_{(t=0)} + [Py^*_{diff}]_{(t=0)} e^{-A_3} \sum_{i=0}^{\infty} \frac{{A_3}^i}{i!} \frac{A_2 + iA_4}{\frac{1}{\tau_M} - \frac{1}{\tau_{E0}} + A_2 + iA_4}\right) e^{-t/\tau_{E0}} + [D^*]_{(t=0)} e^{-t/\tau_D} \quad (4)$$

Equation 4 was used to fit the excimer decays. In eq 4, $[Py^*_{diff}]_{(t=0)}$, $[E0^*]_{(t=0)}$, and $[D^*]_{(t=0)}$ represent the equilibrium concentrations of the pyrenes which form excimer via diffusion, are preassociated and form an excimer upon direct excitation, and are preassociated and form a long-lived excimer upon absorption of a photon, respectively. The lifetimes of E0* and D* are τ_{E0} and τ_D, respectively. The procedure used to fit the excimer decays with eq 4 has been described in earlier publications.[21−23]

Viscosity Measurements. The pyrene-labeled EP-MAH was dissolved in 10 mL of hexane. The solution was stirred for at least 24 h before performing the viscosity measurements with an Ubbelohde viscometer at 25 ± 0.1 °C.

Förster Radius Determination. Np and Py are two dyes which form excimer. This property complicates the determination of the Förster radius (R_o) because the emission of the donor (Np) is quenched via excimer formation reducing the fluorescence quantum yield of the donor (Q_D) and the absorption spectrum of the acceptor (Py) is distorted by the presence of ground-state dimers generated during the labeling reaction affecting the extinction coefficient of the acceptor (ϵ_A).[31] To minimize the process of excimer formation, a maleated oligoisobutylene (OIB-MAH) was used where 79% of the SAH moieties were attached as single units onto the chains.[32] OIB-MAH was reacted with PMA or NMA as previously done with EP-MAH to yield a Py-labeled (Py-OIB) or Np-labeled (Np-OIB) oligoisobutylene, respectively.[32] The fluorescence spectra were acquired by exciting optically dilute (OD < 0.1) samples of Np-OIB and Py-OIB at 265 and 344 nm, respectively. The spectra showed the characteristic features of the pyrene and naphthalene monomers with a small tail at longer wavelengths which indicated the residual presence of excimer due to the 21% of SAH units which had attached in a clustered manner onto the OIB chains (cf. Figure S1 in Supporting Information). Comparison of the Np fluorescence spectrum acquired on the PTI fluorometer with that reported in ref 33a led to the conclusion that no wavelength induced correction needed to be made to the Np fluorescence spectra. The excimer-free fluorescence spectrum of the naphthalene monomer was determined by noting that the last band of the naphthalene spectrum located at 350 nm was very similar to that of the Np-OIB spectrum. The excimer-free tail of the naphthalene fluorescence spectrum was used to replace that of the Np-OIB

spectrum. This procedure allowed us to obtain the fluorescence spectrum of the excimer-free naphthalene monomer of Np-OIB in THF and hexane.

The quantum yield of the naphthalene monomer of Np-OIB (Q_D^{Np-OIB}) in hexane and THF was determined by comparison with that of the reference (naphthalene in cyclohexane, $Q_D^{ref} = 0.23$)[33a] and using eq 5.[34]

$$Q_D^{Np-OIB} = Q_D^{ref}\left(\frac{Abs_{ref}(\lambda_{ex})}{Abs_{Np-OIB}(\lambda_{ex})}\right)\left(\frac{n_{solvent}}{n_{cyclohexane}}\right)^2\left(\frac{\int_0^\infty F^M_{Np-OIB}(\lambda)\,d\lambda}{\int_0^\infty F_{ref}(\lambda)\,d\lambda}\right) \quad (5)$$

In eq 5, $n_{solvent}$ is the refractive index of the solvent in which the fluorescence spectra of Np-OIB are acquired. It equals 1.4070, 1.3749, and 1.4260 for THF, hexane, and cyclohexane, respectively. The integral $\int_o^\infty F(\lambda)\,d\lambda$ represents the integrated area under the fluorescence spectrum. The index M in $F^M_{Np-OIB}(\lambda)$ indicates that the fluorescence spectrum of Np-OIB has been altered to obtain the spectrum of the excimer-free naphthalene monomer. Q_D^{Np-OIB} was found to equal 0.10 both in THF and hexane. This value is smaller than or close to those found for 1-methylnaphthalene (0.25 in cyclohexane,[33b] 0.18 in toluene,[35] 0.12 in 95% ethanol,[35] 0.11 in water at pH 7).[36] The lower quantum yields obtained for Np-OIB in THF and hexane might be a result of the proximity of the polar succinimide moiety to Np and the fact that 21% of all Np are attached onto clustered SAH units enabling excimer formation and quenching of the Np monomer.

R_o was determined from the donor−acceptor spectral overlap integral using eq 6[26c]

$$R_o = 0.211\left[\kappa^2 n^{-4} Q_D \frac{\int_0^\infty F^M_{Np-OIB}(\lambda)\epsilon_{Py-OIB}(\lambda)\lambda^4\,d\lambda}{\int_0^\infty F^M_{Np-OIB}(\lambda)\,d\lambda}\right]^{1/6} \quad (6)$$

where ϵ_{Py-OIB} is the extinction coefficient of the pyrene monomer. The factor κ^2 represents the relative orientation in space of the transition dipole moments of the donor and acceptor and was taken to equal $^2/_3$ assuming a dynamic random averaging of the orientations of the donor and acceptor dipole moments. R_o was found to equal 34 and 35 Å in hexane and THF, respectively. This value is slightly larger than the values of 29 Å obtained for the 1-methylnaphthalene and pyrene pair[37] and two naphthalene- and pyrene-labeled polymers.[38]

Results and Discussion

The purpose of this work is to determine whether a minute amount of grafted MAH (1.5 wt %) is attached to an EP copolymer as isolated or clustered units. The challenge consists of selecting a technique capable of providing structural information on so small a fraction of the entire polymer matrix. The sensitivity of fluorescence makes it an ideal candidate to carry out this study. Fluorescence provides structural information at the molecular level by using dyes which can either form excimer[26b] or undergo fluorescence resonance energy transfer (FRET).[26c] Consequently this manuscript is organized as a series of experiments which use different aspects of fluorescence. The fact that the conclusions about the microstructure of the EP-MAH drawn from this set of independent experiments concur, brings confidence that such measurements can be applied toward the determination of the microstructure of EP-MAH.

Pyrene-Labeled EP Copolymers. The parameters characterizing the two polymers EP-I and EP-II prior to labeling are listed in Table 1. Both EP-MAHs contain about one grafted MAH unit per 200 polymeric units, a very low level of grafting as is often the case for EP-MAH.[9f,39] The pyrene (Py) content λ (μmol/g) determined by UV−vis absorption provided the average number of backbone units per Py and both parameters are listed in Table 2. The labeling reactions were carried out in duplicate (R1 and R2) to determine the reproducibility of these experiments. For both EP samples, the Py content is obtained reproducibly within experimental error (less than 4%) for the two labeling reactions. The average Py content for all four Py-EP samples equals 160 ± 10 μmol/g which is in agreement with the overall MAH content of both maleated EP copolymers (149 ± 2 μmol/g). Small discrepancies observed between Py and MAH content may be expected, since different techniques were used for their characterization.

Scheme 3

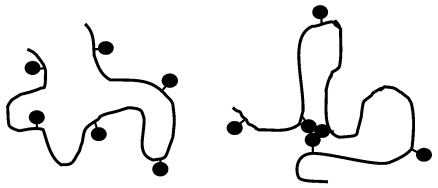

The Py-EPs were studied by UV−vis absorbance and fluorescence in THF and hexane to obtain information about their conformation. For short EP copolymers, the polar THF can solubilize the EP copolymer backbone, the succinimide moieties, and Py. The apolar hexane, on the other hand, will solubilize the EP backbone and the aromatic Py to some extent, but not the succinimide moieties. As a result, polar associations between the succinimide moieties as well as potential $\pi-\pi$ interactions between the Py units will take place in hexane. Scheme 3 shows the expected conformations of Py-EP in THF and hexane. The solid disks represent the 1-pyrenemethylsuccinimide pendants.

Absorption measurements performed on Py-EP solutions can provide qualitative information about the level of aggregation between Py pendants. A broadening of the absorption bands is usually observed as a result of Py association.[31] The peak-to-valley ratio, P_A, provides a measure of this broadness by measuring the ratio of the absorbance of the peak at 344 nm to that of the nearest valley. A P_A value of 3.0 or above indicates absence of association. The P_A value decreases with increasing levels of Py association. The P_A values equal 3.2 ± 0.1 and 1.9 ± 0.1 for Py-EP-I in THF and hexane, respectively. For Py-EP-II, P_A yields values of 2.8 ± 0.1 and 1.9 ± 0.0 in THF and hexane, respectively. For either Py-EP, the P_A value is lower in hexane than in THF, indicating that more Py aggregates exist in hexane than in THF. This is a result of the dipolar associations in hexane taking place between the polar succinimide pendants resulting from the attachment of 1-pyrenemethylamine onto EP-MAH. The P_A values listed in Table 2 are in excellent agreement with those reported for another Py-EP.[19] Interestingly, Py-EP-II yields lower P_A values than Py-EP-I in THF. Given the fact that dipolar associations induced by the succinimide moieties are expected to be strongly reduced in THF, the smaller P_A values obtained for Py-EP-II indicate that the Py groups are distributed on Py-EP-II in a more clustered manner than on Py-EP-I. Since the Py dyes are attached at the SAH moieties grafted onto the EP

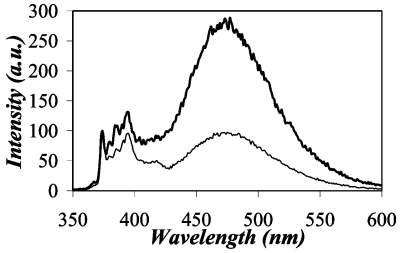

Figure 2. Fluorescence emission spectra of Py-EP-II-R2 acquired in hexane (—) and in THF (−). $\lambda_{ex} = 344$ nm.

backbone, the Py clustering on EP-II reflects a more clustered distribution of the SAH moieties on EP-II than on EP-I.

In a fluorescence experiment, UV light is shone onto the Py-EP solution to excite the Py monomer. The excited monomer can either emit a photon at a rate $k_M = \tau_M^{-1}$, where τ_M is the lifetime of the Py monomer, or it can form an excimer upon encounter with a ground-state Py. The Py monomer fluorescence emission exhibits sharp peaks between 370 and 410 nm, whereas that of the excimer is broad and structureless around 480 nm (cf. Figure 2). Since the process of excimer formation depends on the average distance separating any two Py units attached on the polymer, an increased excimer formation indicates that the Py units are closer to one another.

Steady-state fluorescence spectra of Py-EP in THF and hexane were acquired using an excitation wavelength of 344 nm. They are shown in Figure 2 for Py-EP-II-R2. The monomer intensity (I_M) refers to the intensity integrated between 372 and 378 nm, while the excimer intensity (I_E) refers to the intensity integrated between 500 and 530 nm. The ratio I_E/I_M gives information about the extent of Py excimer formation for a given polymer/solvent system. Figure 2 describes the effect of the solvent on the fluorescence spectra of Py-EP. The I_E/I_M values are smaller in THF than in hexane. They are listed for all polymer/solvent combinations in Table 3 and indicate that less Py excimer is formed in THF than in hexane. These results are expected because hexane, being a poor solvent for the polar succinimide moieties, induces them to associate. These dipolar associations lead to the formation of Py aggregates where the Py local concentration is very high and excimer formation is efficient.

The existence of Py aggregates can be further supported by performing fluorescence excitation spectra. Excitation spectra were monitored using an emission wavelength of 375 and 500 nm for the Py monomer and excimer, respectively. The observation of a shift between the monomer and excimer excitation spectra indicates the presence of ground-state Py dimers. Since noticeable shifts between the monomer and excimer excitation spectra are observed in hexane, more ground-state Py dimers are formed in hexane than in THF (cf. Figure 3). The same trend is observed for both Py-EP-I and Py-EP-II.

The I_E/I_M ratios listed in Table 3 also allow comparisons to be made between Py-EP-I and Py-EP-II. Although Py-EP-II exhibits a slightly lower Py content than Py-EP-I (cf. Table 2), the I_E/I_M ratio for Py-EP-II in THF and in hexane is always larger than that of Py-EP-I. Since closer Py units will form more excimer, this result shows that the Py moieties are distributed in a more clustered manner on EP-II than on EP-I.

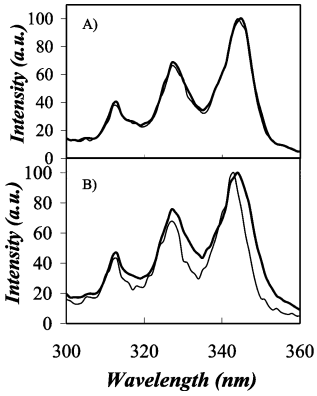

Figure 3. Fluorescence excitation spectra of Py-EP-I in (A) THF and (B) hexane: $\lambda_{em} = 375$ nm (−); $\lambda_{em} = 500$ nm (—).

Time-resolved fluorescence decays of the Py monomer and excimer were acquired for both polymers in THF and hexane to confirm the trends observed by steady-state fluorescence. All fluorescence decays were acquired with polymer solutions having a Py concentration of 2.5×10^{-6} M. The parameters obtained by fitting the fluorescence decays of the Py monomer and excimer with a multiexponential function are listed in Table 4, parts A and B, respectively. The longer decay time of the Py monomer was fixed to that of a Py unit attached at one end of an oligoisobutylene. The lifetime of this model compound was found to equal 290 ns in THF and 350 ns in hexane.[32] To get satisfying χ^2 (smaller than 1.3), four exponentials were needed to fit the monomer decays. The excimer decays could be fitted with a sum of three exponentials. The results from the triexponential fit of the excimer decays were used to gain qualitative information about the level of clustering of the Py pendants.

All excimer decays except the one obtained for Py-EP-II-R2 in hexane show a short rise time, which was taken into account by the first exponential. The second and third exponentials exhibit positive preexponential factors. For all decays, the fraction $a_{e2}/(a_{e2} + a_{e3})$ equals 0.90 ± 0.03. The second decay time τ_{e2} equals 71 ± 3 and 65 ± 2 ns in THF and hexane, respectively. The third and longest decay time τ_{e3} was obtained with less accuracy, because the fraction $a_{e3}/(a_{e2} + a_{e3})$ is small (0.10 ± 0.03). It equals 158 ± 13 and 145 ± 12 ns in THF and hexane, respectively. The presence of the long decay time in the excimer decays has been observed in numerous other instances[18,21−23] and has been attributed to the presence of long-lived Py aggregates (D* in eq 4) as reported in other studies.[40]

In a Py excimer decay, the presence of a rise time results in a negative preexponential factor a_{e1} and two positive preexponential factors a_{e2} and a_{e3}. The ratio $\xi = a_{e1}/(a_{e2} + a_{e3})$ can yield information about the formation mechanism of the Py excimer. In particular, ξ can equal 0 or −1 in cases where the Py excimer is formed exclusively via preassociated ground-state dimers or via diffusive encounters, respectively. For a typical solution of a Py-labeled polymer, both mechanisms are involved. As a consequence, ξ yields values ranging between −1 and 0, depending on the fraction of Py excimer formed by one mechanism against the other. A more positive value indicates that more Py units are preassociated. In THF, Py-EP-I and Py-EP-II take ξ values equal to -0.61 ± 0.03 and -0.40 ± 0.02, respectively. According to these results, Py-EP-II exhibits more preassociated Py units than Py-EP-I. In hexane where dipolar as-

sociations between the succinimide moieties are present, both Py-EP-I and Py-EP-II take much more positive ξ values, which equal -0.28 ± 0.02 and -0.01 ± 0.04, respectively. This confirms the qualitative observation made with the UV−vis absorption measurements (cf. P_A values in Table 2) and the steady-state fluorescence excitation spectra (cf. Figure 3), namely that associations between the succinimide moieties are much stronger in hexane than in THF. It is worth pointing out that Py-EP-II always yields more positive ξ values than Py-EP-I, regardless of the solvent, even though the Py contents of both polymers are similar (cf. Table 2). The analysis of the excimer fluorescence decays indicates that a higher fraction of preassociated ground-state Py is present in Py-EP-II than in Py-EP-I, reflecting a more clustered attachment of the SAH moieties.

The increase in association observed in hexane vs in THF does not arise from hexane being a poorer solvent toward the EP backbone, which would lead to an increase in the local concentration of pendants in the polymer coil and an enhanced level of association. Intrinsic viscosity measurements carried out in hexane and THF on the naked EP copolymer yielded values of 1.06 and 0.85 dL/g, respectively (cf. Figure S2 in the Supporting Information). These results demonstrate that hexane is a better solvent than THF toward the EP backbone. This statement also agrees with the solubility parameter values of 14.9,[41] 18.6,[41] and 15.7[42] $MPa^{1/2}$ available in the literature for hexane, THF, and an EP rubber, respectively. Thus, the excess intramolecular association observed in hexane for the modified polymers is a result of the poor solubility of the succinimide pendants in that solvent.

The results described for the Py-EPs indicate that these Py-labeled polymers behave in exactly the same manner as the Py-labeled poly(L-glutamic acid),[21] poly(*N,N*-dimethylacrylamide),[22] hydrophobically modified alkali swellable emulsion polymers,[23] and other Py-EPs studied earlier in this laboratory[18] and others.[19] Consequently, the procedures established by this laboratory to study Py-labeled polymers are expected to hold with the present system.[21−23] This analysis is being conducted in the third part of this article.

Doubly Labeled EP Copolymers. Fluorescence resonance energy transfer (FRET) is used as a "spectroscopic ruler" exploiting the strong dependence of the FRET efficiency on the distance separating a donor from an acceptor.[43] The dyes chosen for our experiments were Np and Py. The Np/Py pair is used routinely for FRET experiments, where the donor Np can be excited selectively and the energy transfer from the excited Np* to the ground-state Py can be monitored by steady-state or time-resolved fluorescence.[44,45]

Several doubly labeled EP copolymers with different Py-to-Np ratios were prepared. Their overall dye content and percentage of Py labeling is listed in Table 5. The fraction of Py attached onto the polymers ranged from 0 to 43%. Some labeling reactions yielded a 25% lower than expected overall dye content, such as for Py40-Np60-EP-I. At this stage, no explanation can be found to rationalize this 25% reduction in labeling efficiency.

The steady-state fluorescence measurements of the doubly labeled polymers in THF were conducted. Upon excitation at 290 nm, strong Py emission was observed in Figure 4 in comparison with the weak Py emission of the Py-EPs obtained at the same Py concentration. At the same time, the Np emission is significantly reduced with respect to that of Np-EP obtained at the same Np concentration. Figure 4 demonstrates that the enhancement of the Py emission is achieved at the cost of the Np emission when the doubly labeled polymer sample is excited at 290 nm.

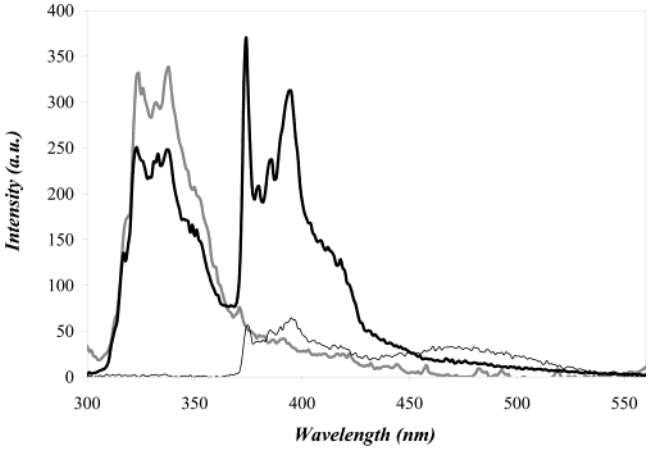

Figure 4. Emission spectra of EP-II in THF (λ_{ex} = 290 nm): Np-EP-II (thick gray line); Py11-Np89-EP-II (thick black line); Py-EP-II (thin black line). The Py and Np concentrations equal 2.2×10^{-6} and 1.8×10^{-5} M, respectively.

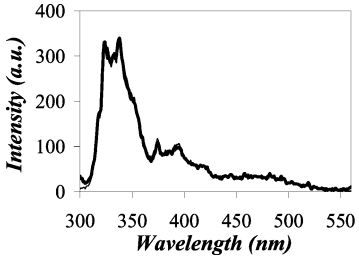

Figure 5. Emission spectra of mixing experiment in THF (λ_{ex} = 290 nm): (i) mixed solution of Py-EP-II and Np-EP-II (−) and (ii) addition of the fluorescence spectrum of Py-EP-II alone with that of Np-EP-II alone (—). Concentrations: 2.2×10^{-6} M (Py-EP-II); 1.8×10^{-5} M (Np-EP-II).

To determine whether FRET occurs between chromophores attached to the same chain or to different chains, i.e., intra- vs interchain FRET, emission spectra were acquired for solutions containing Py-EP-II, Np-EP-II, and a mixture of the two. The solutions were prepared so that the concentration of Py or Np would equal 2.2×10^{-6} or 1.8×10^{-5} M, respectively. When the mixed solution of Py-EP-II and Np-EP-II was excited at 290 nm, an emission spectrum with a very weak contribution from the Py monomer (emission at 374 nm) and a strong contribution from Np (emission at 330 nm) was obtained (cf. Figure 5). The comparison of this emission spectrum with the sum of the individual spectra of Py-EP-II and Np-EP-II shows little difference, demonstrating that no FRET occurs between two chromophores located on different chains. This result was observed for both polymers in THF and hexane (cf. Figures S3A−C in Supporting Information). Consequently, the conclusion is that no polymer/solvent combination leads to any interpolymeric association in the range of polymer concentrations used in the fluorescence experiments.

Steady-state fluorescence spectra were recorded in THF and hexane for all doubly labeled EP copolymers and trends similar to those shown in Figure 4 were obtained. These spectra can be used to qualitatively describe the extent of FRET by the ratio between the

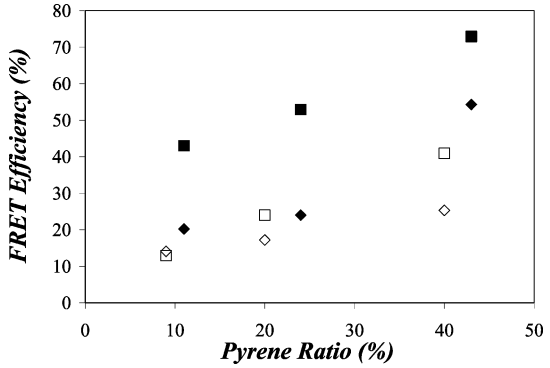

Figure 6. FRET efficiency for doubly labeled EP-I in THF (◇) and hexane (□) and doubly labeled EP-II in THF (◆) and hexane (■).

Py intensity integrated between 372 and 378 nm (I_{375}) and the Np intensity integrated between 320 and 326 nm (I_{323}). The I_{375}/I_{323} ratios are listed in Table 5. They indicate that the extent of FRET increases with Py content, increases when changing solvent from THF to hexane, or increases when using EP-II vs EP-I. These trends were quantified by calculating the FRET efficiencies.

The efficiency of FRET was calculated as follows. The intensity of the Np emission (I_{Np}) was determined for each sample. It was compared to the fluorescence intensity of the corresponding Np-labeled polymer (I^{o}_{Np}) and divided by the Np concentration in each sample. The ratio between the two normalized emissions, $\{I_{Np}/[Np]\}/\{I^{o}_{Np}/[Np°]\}$, was obtained. The efficiency of FRET (E) was calculated using eq 7. In all experiments, the absorbance of the solution at the excitation wavelength and at larger wavelengths was kept below 0.1 to minimize the inner filter effect and to prevent reabsorption by the acceptor.[25a,c]

$$E = 1 - \frac{I_{Np}/[Np]}{I^{o}_{Np}/[Np^{o}]} \qquad (7)$$

The FRET efficiency for the samples is shown in Figure 6. In either THF or hexane, increasing the Py-to-Np ratios yields higher FRET efficiencies. Furthermore, as the Py-to-Np ratio increases, more Py units are located close to one another and Py excimers are observed at higher Py contents, the effect being more pronounced in hexane. This effect is not expected to affect the efficiency of FRET, which is calculated with the Np fluorescence spectra. In either solvent, the FRET efficiency of the doubly labeled EP-II is larger than that of EP-I even though their Py contents are very close. This trend further supports the notion that EP-II has a higher level of succinimide clustering than EP-I, in agreement with the earlier conclusions obtained with the Py-EPs.

Fluorescence decays of the doubly labeled polymer samples were measured to gain further information on how FRET occurs. The Np monomer decays were fitted with a triexponential function. The parameters obtained from the analysis are listed in Table S1 in the Supporting Information. The Np fluorescence decays were found to be nonexponential. The nonexponentiallity of the decays is due to the ability of Np to form an excimer and/or to undergo FRET when a Py molecule is nearby, two processes which complicate the shape of the fluorescence decays.

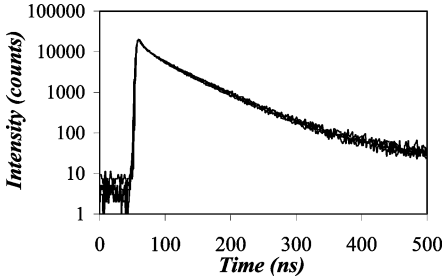

Figure 7. Fluorescence decays of doubly labeled EP-II in hexane (excited at 290 nm, monitored at 338 nm). The fractions of dyes which are Py are 0, 11, 24, and 43 mol %. The overlap of the four traces is excellent.

For each polymer/solvent combination, the Np decays acquired with increasing Py content were normalized at the decay maximum. As shown in Figure 7, the fluorescence decays of the doubly labeled EP-II in hexane are found to overlap. A similar trend is observed in THF (cf. Figure S4C in Supporting Information).

The lack of effect that increasing levels of Py labeling have on the fluorescence decays contrasts sharply with the evidence obtained by steady-state fluorescence that efficient FRET is taking place for the doubly labeled EP-II in THF or hexane (cf. I_{375}/I_{323} in Table 5 and the FRET efficiency in Figure 4). The discrepancy observed between the steady-state and time-resolved fluorescence experiments can only be rationalized if the dyes are clustered. Since the rate of energy transfer depends on the inverse of the distance separating the donor (Np) and the acceptor (Py) to the sixth power,[25c] FRET occurs on a very fast time scale if Np and Py are located close to each other. Clustering of the dyes implies a highly efficient FRET, as observed by steady-state fluorescence, but occurring on a time scale too rapid to be probed by our nanosecond time-resolved fluorometer. This effect has already been observed.[46] Consequently, the fluorescence decays depict those Np units which are not close to the Py dyes and behave in a manner similar to the Np units attached onto Np-EP-II. On the other hand, the fluorescence decays obtained with the doubly labeled EP-I in THF and hexane exhibit some spread, which indicates that the dyes are less clustered in EP-I (cf. Figure S4, parts A and B in the Supporting Information).

To support the notion that some naphthalene and pyrene pairs are so close that the rate of energy transfer is too large to be detected by our instrument, efforts were made to estimate the distance separating a pair of dyes attached on two successive units of an EP chain. The microstructure **III** shown in Scheme 1 is obtained when the attachment of a MAH moiety onto a propylene unit leads to further MAH grafting onto nearby propylene units, leading to clustering of the SAH pendants along the EP backbone. To find an estimate of the distance between a Np and Py dyes attached onto two consecutive propylene units, molecular mechanics optimizations were carried out using the Fletcher−Reeves algorithm on 4-methyl,6-methyl,4−1-pyrenemethylsuccinimide,6−1-naphthalenemethylsuccinimide decane (Py-Np-decane, cf. Figure 8a). The molecule was created with the program Hyperchem (release 7.02 for Windows). The geometry of the molecule was optimized by imposing that the distances between the Np and Py carbon atoms $C_1^{Np}-C_1^{Py}$, $C_3^{Np}-C_7^{Py}$, and $C_6^{Np}-C_7^{Py}$ would vary by 1-Å steps between 3 and 14 Å, 3 and 24 Å, and 3 and 25 Å, respectively. The energy of the

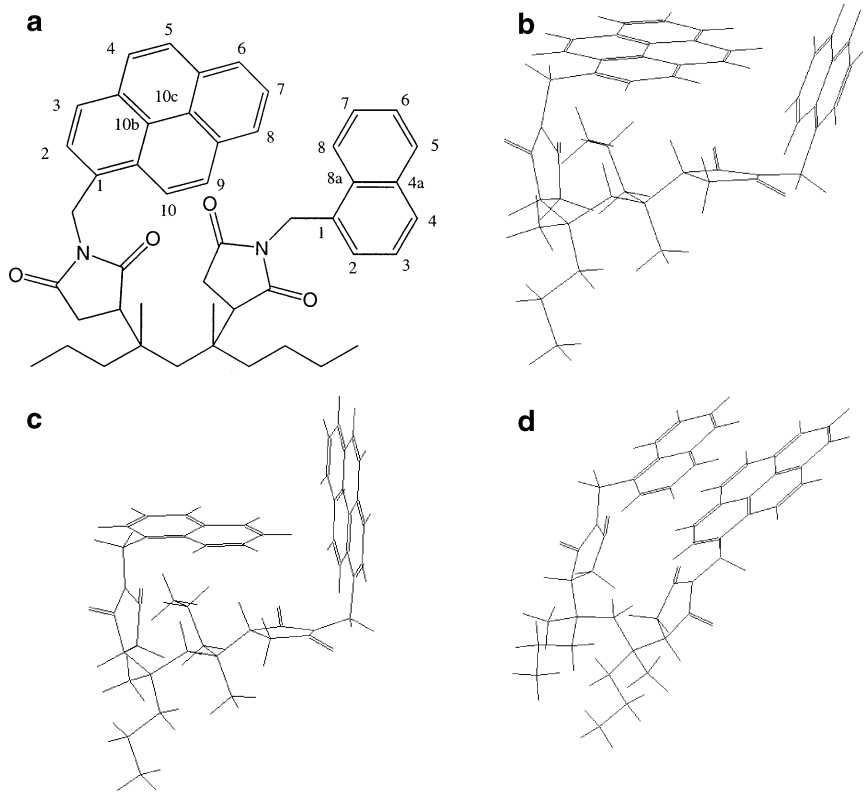

Figure 8. (a) 4-Methyl-6-methyl-4−1-pyrenemethylsuccinimide-6−1-naphthalenemethylsuccinimidedecane. (b) Structure obtained at the energy minimum ($d(C_3^{Np}-C_7^{Py}) = 4.9$ Å, $E = 45.5$ kcal). (c) Structure obtained at the energy minimum ($d(C_6^{Np}-C_7^{Py}) = 8$ Å, $E = 47.6$ kcal). (d) Structure obtained at the energy minimum ($d(C_1^{Np}-C_1^{Py}) = 4$ Å, $E = 44.5$ kcal).

molecule was recorded at each step. It passed through a minimum over the range of distances probed (cf. Figure S5 in Supporting Information). The structures obtained at the energy minima are shown in Figure 8b−d. Certainly numerous other structures can be found. The set of structures shown in Figure 8b−d is to demonstrate that the Py-Np-decane molecule can adopt energetically stable conformations where the two dyes are very close to one another.

Py-Np-decane mimics an EP chain where two consecutive propylene units are grafted with MAH and labeled with 1-pyrenemethylamine and 1-naphthalenemethylamine. The structures with the lowest energy were found when Py, Np, and the two succinimide moieties form the side of a square. The structure with the best overlap between Np and Py exhibits the lowest energy (cf. Figure 8d). The structure in Figure 8b exhibits some $\pi-\pi$ stacking between the carbonyl of the succinimide and the carbons C_4, C_5, and C_6 of the Py moiety. In Figure 8c, Np is not able to π-stack with the carbonyl of the succinimide because its smaller size prevents it to reach. Unsurprisingly, the structure in Figure 8c has the highest energy. An estimate of the center-to-center distance between naphthalene and pyrene (d) was obtained from eq 8.

$$d = \frac{d(C_{10b}^{Py}-C_{8a}^{Np}) + d(C_{10c}^{Py}-C_{8a}^{Np}) + d(C_{10b}^{4a}-C_{4a}^{Np}) + d(C_{10c}^{Py}-C_{4a}^{Np})}{4} \quad (8)$$

The distance d was found to equal 6.3, 6.2, and 4.1 Å for the structures shown in Figure 8, parts b, c, and d, respectively. The decay time τ_{FRET} for FRET taking place between Np and Py is obtained from the relationship $((1/\tau_{Np}) + (1/\tau_{Np})((R_o/d))^6)^{-1}$ where R_o equals 34 and 35 Å in hexane and THF, respectively (cf. Experimental section). The average lifetime (τ_{Np}) of Np-EP equals 42 ± 1 and 33 ± 3 ns in THF and hexane, respectively (cf. Table S1 in Supporting Information). The distance d obtained for the structures shown in Figure 8, parts b, c, and d yields τ_{FRET} values which are smaller than 2 ps, a process which cannot be detected by the PRA time-resolved fluorometer used in this study. These molecular mechanics optimizations combined with the FRET results strengthen the notion that a substantial fraction of the SAH units are attached in a clustered manner on the EP backbone.

Quantitative Determination of the Level of Clustering. Since all experiments performed with both Py-EPs indicate that these polymers behave in a manner similar to that of other Py-labeled polymers,[18,21−23] the blob model which was applied to determine the level of pyrene clustering can be used with both Py-EPs. The blob model was introduced to account for the distribution of excimer formation rate constants, which results from the random attachment of Py units along a polymeric backbone. In the analysis, the fluorescence decays of the Py monomer are fitted with eq 2 to obtain the fraction of Py monomers which are isolated ($f_{Mfree} = 1-f$) or form excimer via diffusion ($f_{Mdiff} = f$). The analysis of the monomer fluorescence decays also retrieves the parameters $\langle n \rangle$, k_{blob}, and k_e[blob] which model the diffusive encounters between an excited Py group and a ground-state Py or Py dimer. These three parameters are then fixed in eq 4 to analyze the excimer fluorescence decays. This procedure is introduced to restrain the number of adjustable variables. Analysis of the excimer decays yields the fraction of Py units which form excimer via either diffusion (f_{Ediff}), ground-state dimers E0 (f_{EE0}), or D (f_{ED}). The fractions f_{free}, f_{diff},

Table 6.

A. Parameters Retrieved from the Blob Model Analysis of the Py Monomer Decays of Py-Labeled EP-MAHs

sample	λ (μmol/g of polymer)	solvent	f_{Mdiff}	f_{Mfree}	k_{blob} (10^7 s^{-1})	k_{ex}[blob] (10^6 s^{-1})	$\langle n \rangle$	τ_M (ns)	χ^2
Py-EP-I-R1	170	THF	0.89	0.11	1.6	3.4	1.4	290	1.01
Py-EP-I-R2	166		0.87	0.13	1.7	4.3	1.4	290	1.15
Py-EP-II-R1	150		0.91	0.09	1.4	2.8	1.5	290	1.10
Py-EP-II-R2	163		0.90	0.10	1.8	3.5	1.4	290	1.12
Py-EP-I-R1	170	hexane	0.83	0.17	1.7	4.8	1.3	350	1.10
Py-EP-I-R2	166		0.82	0.18	2.3	5.0	1.4	350	1.16
Py-EP-II-R1	150		0.96	0.04	1.7	3.7	1.4	350	1.17
Py-EP-II-R2	163		0.88	0.12	1.3	2.6	1.4	350	1.17

B. Parameters Retrieved from the *Blob* Model Analysis of the Py Excimer Decays of Py-Labeled EP-MAHs

sample	λ (μmol/g of polymer)	solvent	f_{Ediff}	f_{EE0}	f_{ED}	τ_{E0} (ns)	τ_D (ns)	χ^2
Py-EP-I-R1	170	THF	0.66	0.30	0.04	65	158	1.10
Py-EP-I-R2	166		0.66	0.30	0.04	63	158	1.05
Py-EP-II-R1	150		0.47	0.50	0.03	67	158	1.14
Py-EP-II-R2	163		0.49	0.47	0.04	59	158	1.17
Py-EP-I-R1	170	hexane	0.33	0.59	0.08	64	145	1.20
Py-EP-I-R2	166		0.37	0.58	0.05	59	145	1.09
Py-EP-II-R1	150		0.01	0.94	0.05	63	145	0.99
Py-EP-II-R2	163[a]							

C. Fraction of Associated Py Units f_{agg} ($=f_{E0}+f_D$)

sample	solvent	f_{diff}	f_{free}	f_{E0}	f_D	f_{agg}
Py-EP-I	THF	0.61 ± 0.01	0.08 ± 0.01	0.28 ± 0.02	0.03 ± 0.01	0.34 ± 0.01
Py-EP-II		0.46 ± 0.00	0.05 ± 0.00	0.46 ± 0.02	0.03 ± 0.01	0.51 ± 0.00
Py-EP-I	hexane	0.33 ± 0.02	0.07 ± 0.01	0.54 ± 0.01	0.06 ± 0.02	0.65 ± 0.03
Py-EP-II		0.01	0	0.94	0.05	0.99

[a] No rise time; the analysis cannot be carried out due to the lack of rise time in the excimer decay.

f_{E0}, and f_D representing, respectively, the populations Py_{free}, Py_{diff}, *E0*, and *D* are obtained by combining f_{Mfree}, f_{Mdiff}, f_{Ediff}, f_{EE0} and f_{ED} according to an established procedure.[21−23] The fraction of associated Py units (f_{agg}) is obtained by summing f_{E0} and f_D. A recent study carried out on a Py-labeled poly(L-glutamic acid) in DMF confirmed the validity of this approach to determine the level of association between Py groups randomly attached onto a polymer.[21]

The lifetimes of the excited species Py* (τ_M), E0* (τ_{E0}), and D* (τ_D) were determined in the following manner. In the case of τ_M, an earlier study showed that 1-pyrenemethylamine attached onto an oligoisobutylene via a SAH group at one end exhibits a lifetime of 290 and 350 ns in THF and hexane, respectively.[32] These values were assigned to τ_M for Py-EP in THF and hexane. In the case of the long-lived low energy excited dimers D*, the third decay time (τ_{e3}) obtained from the triexponential fit of the excimer fluorescence decays (cf. Table 4B) has been assigned to τ_D as done in earlier studies. Taking the average of the τ_{e3} values obtained from the triexponential fit of the four excimer decays in THF and hexane, one finds that τ_D equals 158 and 145 ns in THF and hexane, respectively. The lifetime τ_{E0} is optimized in the analysis of the excimer decays.

The parameters f_{Mfree}, f_{Mdiff}, $\langle n \rangle$, k_{blob}, and k_e[blob] obtained from the analysis of the monomer decays are listed in Table 6A. The parameters f_{Ediff}, f_{EE0}, f_{ED}, and τ_{E0} obtained from the analysis of the excimer decays are listed in Table 6B. Table 6C summarizes the results obtained for f_{agg}. The fits of the fluorescence decays were good, since the χ^2 was always smaller than 1.20, and the residuals and the autocorrelation function of the residuals were randomly distributed around zero. Within experimental error, all monomer fluorescence decays yielded similar parameters in THF or hexane with f_{Mfree}, f_{Mdiff}, $\langle n \rangle$, k_{blob}, and k_e[blob] found to equal 0.12 ± 0.04, 0.88 ± 0.04, 1.4 ± 0.1, 1.7 ± 0.3 × 10^7, and 3.8 ± 0.9 × 10^6 s^{-1}, respectively. The lifetime τ_{E0} was found to equal 62 ± 2 ns in THF or hexane. This τ_{E0} value is reasonable since another Py-labeled EP copolymer yielded τ_{E0} values of 56 ± 1 and 61 ± 1 ns in THF and hexane, respectively.[18b] The main difference between the decays appears in the parameters f_{Ediff}, f_{EE0}, and f_{ED}, which lead to the results shown in Table 6C.

The fraction of aggregated Py units (f_{agg}) in THF equals 0.34 ± 0.01 and 0.51 ± 0.00 for Py-EP-I and Py-EP-II, respectively. The f_{agg} values in hexane equal 0.65 ± 0.03 and 0.99 ± 0.01 for Py-EP-I and Py-EP-II, respectively. The latter values are double those obtained in THF, because hexane is an apolar solvent, which is known to induce dipolar associations between MAH pendants. As a consequence of those dipolar associations, more Py aggregates are formed. It is worthwhile to note that, in either solvents, Py-EP-II always yields a larger f_{agg} value than Py-EP-I even though their Py contents are very close, confirming that more Py units are aggregated in the former than in the latter. Since the distribution of Py in a Py-EP mimics that of MAH in an EP-MAH, the higher level of Py aggregation observed for EP-II demonstrates that EP-II exhibits a more clustered MAH microstructure than EP-I.

Viscosity of EP Copolymer Solutions. Derivatives of maleated EP copolymers are being widely used as engine oil additives. Although the effect of MAH clustering is widely believed to affect the rheological properties of modified EP copolymers in solution, it has not been reported yet in a scientific publication. This is certainly a consequence of the lack of analytical techniques capable of providing information on the distribution of SAH attached onto a polyolefin backbone. The fluorescence experiments carried out earlier on EP-I and EP-II labeled with a set of dyes capable of undergoing either excimer formation or FRET led to the conclusion

Table 7. Molecular Weight, MAH Graft Content, and Py Content of EP Copolymer Samples Used for Viscosity Measurements

polymer sample	M_n (kg/mol)	M_w/M_n	Py content λ (μmol/g of polymer)	f_{agg} in THF	f_{agg} in hexane
Py-EP-I-R2	41 ± 1^a	3.0 ± 0.3^a	166	0.34	0.63
Py-EP-II-R2	40 ± 0^a	2.6 ± 0.3^a	163	0.51	0.99
EP-III	107	1.9	0	0	0

[a] Average value of three GPC runs.

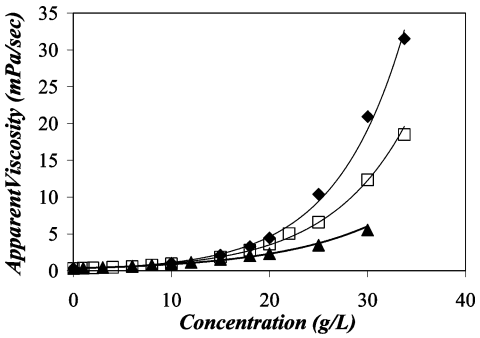

Figure 9. Apparent viscosity of EP copolymers in hexane: (□) Py-EP-I, (◆) Py-EP-II, and (▲) EP-III.

that the succinimide moieties are more clustered in EP-II than in EP-I. Consequently these two polymers, which are similar in all other features (i.e., molecular weight, molecular weight distribution, and ethylene and MAH contents, cf. Table 7) but the distribution of the SAH on the backbone (cf. f_{agg} in THF in Table 7), are good candidates to investigate the effect of SAH clustering on the viscosity of a solution of EP-MAH in oil.

Viscosity measurements of the three EP copolymers were carried out in hexane. Among the three samples, two were Py-labeled (Py-EP-I-R2 and Py-EP-II-R2), whereas the third one was a naked EP copolymer of higher molecular weight referred to as EP-III. Some features of the three polymers are listed in Table 7. Figure 9 shows that the viscosity increases with increasing polymer concentration for all samples. However, the Py-EP samples exhibit a faster viscosity increase than EP-III, even though they have a lower molecular weight.

The viscosity of a polymer solution increases with the fraction of the total volume which is occupied by the polymer coils. Since scaling laws predict that a given mass m_o of a high molecular weight polymer occupies a larger volume fraction than the same mass m_o of a lower molecular weight polymer, the behavior exhibited by Py-EP-I and Py-EP-II in Figure 9 can be rationalized only if Py-EP-I and Py-EP-II occupy a larger volume fraction than EP-III. This is possible only if both polymers form intermolecular polymeric aggregates. This is a reasonable possibility, since the two Py-EP copolymers display polar succinimide moieties which are aggregated in apolar hexane. Furthermore, the trends shown in Figure 8 indicate that over a large concentration range, Py-EP-II with a more clustered distribution of succinimide moieties always exhibits a higher viscosity than Py-EP-I. Following a similar line of reasoning, this trend suggests that Py-EP-II occupies a larger volume fraction than Py-EP-I; i.e., Py-EP-II forms larger polymeric aggregates than Py-EP-I. The question which then arises is whether a higher level of SAH clustering could induce a stronger tendency toward forming larger interpolymeric aggregates.

It has been previously reported for hydrophobically modified water-soluble polymer (HMWSP) that the level of clustering of hydrophobes attached along the backbone plays a profound role in the solution properties of the resulting polymer.[17] HMWSP with clustered hydrophobes have been shown to exhibit a steeper viscosity increase in water with concentration than polymers with isolated hydrophobes. This observation was made despite the fact that these HMWSP had similar molecular weights and contents of hydrophobes. The differences observed in the solution behavior were directly correlated with the level of clustering of the hydrophobes.

As for HMWSP, the viscosity of the Py-EP sample with a clustered succinimide microstructure exhibits a more severe concentration dependence than the one with a less clustered microstructure. It is interesting to note that either in water or apolar solvent, the clustering of associating pendants located along a polymer chain leads to stronger interchain associations.

In their 1994 study, Fendler et al. calculated the Gibbs free energy change for the association of a Py-EP sample.[19] The magnitude of their ΔG value led them to the conclusion that the association of their Py-EP in hexane was too strong to be rationalized by invoking polar association of the succinimide moieties alone. They suggested that the Py-EP association was enhanced by the formation of interpolymeric microcrystalline domains with polyethylene stretches.[47] Yet they did not consider the extent by which the clustering of the succinimide moieties enhances Py-EP association. According to their reported P_A value of 2.7 in THF, their Py-EP would be more alike our Py-EP-II. The higher level of MAH clustering might have induced the unexpectedly strong interpolymeric association reported by Fendler et al.

Conclusions

Two maleated EP copolymers were reacted with fluorescent dyes, namely 1-pyrenemethylamine and/or 1-naphthalenemethylamine. The distribution of the dyes is expected to reflect that of the SAH moieties along the polymer backbone. The fluorescence properties of the dye-labeled EP copolymers were studied in THF and hexane. UV−vis absorption and steady-state and time-resolved fluorescence measurements carried out on the Py-labeled EP-I and EP-II copolymers led to the conclusion that the dyes were more clustered on EP-II than on EP-I. This conclusion was supported by carrying out FRET measurements on the doubly labeled EP copolymers. FRET was found to be more efficient between Np and Py attached onto EP-II than EP-I, indicating that the Np and Py dyes are, in average, closer to one-another in EP-II than in EP-I. The fluorescence decays of the Np monomer were acquired for the doubly labeled EPs with different Py contents. The decay profiles of the doubly labeled EP-II overlapped in either THF or hexane. This strongly suggests that FRET occurs on a very fast time scale which cannot be probed by our instrument. It indicates a rapid FRET process between Np and Py dyes close to one-another which is certainly due to the clustering of the dyes in EP-II. Molecular mechanics optimizations were made that further support this conclusion.

The fluorescence decays of the Py-labeled EP copolymers were analyzed with the blob model to determine quantitatively the fraction of aggregated Pys. In THF,

which is a good solvent for the succinimide moieties, 34% of all Pys were aggregated in EP-I compared with 51% in EP-II. In the apolar hexane, which induces polar associations between the succinimide moieties, 65% of all Pys were aggregated in EP-I in contrast to 99% in EP-II. This analysis confirmed the conclusion obtained in the qualitative studies of the dye-labeled EP copolymers, which is that EP-I has a lower level of Py clustering than EP-II. Therefore, MAH is less clustered on EP-I than on EP-II.

The rheological properties of the Py-labeled EP copolymers solutions in hexane were investigated by performing viscosity measurements. The viscosity-vs-concentration trends obtained with EP-I and EP-II were compared with that of a third EP copolymer which had not been maleated. The viscosity of both Py-labeled EPs increased faster with polymer concentration than that of EP-III, although the former two have a lower molecular weight than the latter. Moreover, it was found that the viscosity of EP-II increased faster than that of EP-I, suggesting that EP-II forms aggregate at a lower concentration than EP-I. This behavior was found to be analogous to that of HMWSP in aqueous solution and agreed with the notion that a higher clustering of associating pendants on a polymer leads to the formation of larger polymeric aggregates, which are more efficient at hindering the flow of the solution.

This study demonstrates that fluorescence techniques can be applied to characterize the microstructure of maleated EP copolymers and demonstrates how this information can be used to rationalize the rheological properties of these modified EP copolymers in apolar solutions.

Acknowledgment. The authors thank Imperial Oil and NSERC (Canada) for financial support. M.Z. and J.D. acknowledge very helpful discussions with Drs T. White and J. Gao (Imperial Oil). M.Z. and J.D. are indebted to Professor Joao B. P. Soares for using his high temperature GPC instrument. J.D. is thankful for the funding provided by his being awarded a Tier-2 Canada Research Chair.

Supporting Information Available: Table S1, Np fluorescence decay data of doubly-labeled EP-MAHs, Figure S1, fluorescence spectrum of Np-OIB, Figure S2, reduced viscosity measurements as a function of polymer concentration for the naked EP copolymer, Figure S3, emission spectra of the mixing experiment, Figure S4, fluorescence decay of doubly-labeled EP-I and II, and Figure S5, energy (in kcal) vs distance. This material is available free of charge via the Internet at http://pubs.acs.org.

References and Notes

(1) Russell, K. E. *Prog. Polym. Sci.* **2002**, *27*, 1007−1038.
(2) Chung, T. C. *Prog. Polym. Sci.* **2002**, *27*, 39−85.
(3) Moad, G. *Prog. Polym. Sci.*, **1999**, *24*, 81−142.
(4) Chasmawala, M.; Chung, T. C. *Macromolecules* **1995**, *28*, 1333−1339. Immirzi, B.; Lanzetta, N.; Laurienzo, P.; Maglio, G.; Malinconico, M.; Martuscelli, E.; Palumbo, R. *Makromol. Chem.* **1987**, *188*, 951−960; Walch, E.; Gaymans, R. J. *Polymer* **1993**, *34*, 412−417.
(5) Gaylord, N. G. *J. Macromol. Sci.—Rev. Macromol. Chem. Phys.* **1975**, *13*, 235−261. Gaylord, N. G. *CHEMTECH* **1989**, *19*, 435.
(6) Paul, D. R. *Polymer Blends*; Paul, D. R., Newman, S., Eds.; Academic Press: New York, 1978. Liu, N. C.; Baker, W. E.; Russell, K. E. *J. Appl. Polym. Sci.* **1990**, *41*, 2285−2300.
(7) Gerco, R.; Malincohico, M.; Martuscelli, E.; Ragosta, G.; Scarinzi, G. *Polymer* **1987**, *28*, 1185−1189. Pavda, A. R. *Polym. Eng. Sci.* **1992**, *32*, 1703−1710. Hobbs, S. Y.; Bopp, R. C.; Watkins, V. H. *Polym. Eng. Sci.* **1983**, *23*, 380−389.
(8) Jao, T.-C.; Mishura, M. K.; Rubin, I. D.; Duhamel, J.: Winnik, M. A. *J. Polym. Sci., Part B: Polym. Phys.* **1995**, *33*, 1173−1181. Mishra, M. K.; Rubin, I. D. US Patent 5,200,102, 1993.
(9) (a) Gaylord, N. G.; Mehta, M. *J. Polym. Sci., Polym. Lett. Ed.* **1982**, *20*, 481−486. (b) Wu, C. H.; Su, A. C. *Polym. Eng. Sci.* **1991**, *31*, 1629−1636. (c) Wu, C. H.; Su, A. C. *Polym. Eng. Sci.* **1992**, *33*, 1987−1992. (d) Greco, R.; Maglio, G.: Musto, P. V.; Scarinzi, G. *J. Appl. Polym. Sci.* **1989**, *37*, 777−788. (e) Greco, R.: Maglio, G.; Musto, P. V. *J. Appl. Polym. Sci.* **1987**, *33*, 2513−2527. (f) Borsig, E.; Fiedlerova, A.; Hrckova, L. *J. Macromol. Sci.—Pure Appl. Chem.* **1995**, *A32*, 2017−2024. (g) Oostenbrink, A. J.; Gaymans, R. J. *Polymer* **1992**, *33*, 3086−3088. (h) Coutinho, F. M. B.; Ferreira, M. I. P. *Eur. Polym. J.* **1994**, *30*, 911−918. (i) Gaylord, N. G.; Mishra, M. K. *J. Polym. Sci., Polym. Lett. Ed.* **1983**, *21*, 23−30. (j) De Roover, B.; Sclavons, M.; Carlier, V.; Devaux, J.; Legras, R.; Mourtaz, A. *J. Polym. Sci., Part A: Polym. Chem.* **1995**, *33*, 829−842.
(10) (a) Gaylord, N. G.; Mehta, M.: Mehta, R. *J. Appl. Polym. Sci.* **1987**, *33*, 2549−2558. (b) Braun, D.; Eisenlohr, U. *Angew. Makromol. Chem.* **1976**, *55*, 43−57.
(11) Zhu, Y. T.; An, L. J.; Jiang, W. *Macromolecules* **2003**, *36*, 3714−3720.
(12) (a) Tessier, M.: Marechal, E. *Eur. Polym. J.* **1990**, *26*, 499−508. (b) Tessier, M.; Marechal, E. *Eur. Polym. J.* **1984**, *20*, 269−280.
(13) Heinen, W.; Rosemoller, C. H.; Wenzel, C. B.; de Groot, H. J. M.; Lugtenburg, J.; van Duin, M. *Macromolecules* **1996**, *29*, 1151−1157.
(14) Yang, L. Q.; Zhang, F. R.; Endo, T.; Hirotsu, T. *Macromolecules* **2003**, *36*, 4709−4718.
(15) Russell, K. E.; Kelusky, E. C. *J. Polym. Sci., Part A: Polym. Chem.* **1988**, *26*, 2273−2280.
(16) van Duin, M. *Recent Res. Dev. Macromol.* **2003**, *7*, 1−28.
(17) Volpert, E.; Selb, J.; Candau, F. *Macromolecules* **1996**, *29*, 1452−1463. Jimenez-Regalado, E.; Selb, J.; Candau, F. *Langmuir* **2000**, *16*, 8611−8621.
(18) (a) Vangani, V.; Duhamel, J.; Nemeth, S.; Jao, T.-C. *Macromolecules* **1999**, *32*, 2845−2854. (b) Vangani, V.; Drage, J.; Mehta, J.; Mathew, A. K.; Duhamel, J. *J. Phys. Chem. B.* **2001**, *105*, 4827−4839.
(19) Németh, S.; Jao, T.-C.; Fendler, J. H. *Macromolecules* **1994**, *27*, 5449−5456.
(20) Mathew, A. K.; Siu, H.; Duhamel, J. *Macromolecules* **1999**, *32*, 7100−7108.
(21) Duhamel, J.; Kanagalingam, S.; O'Brien, T.; Ingratta, M. *J. Am. Chem. Soc.* **2003**, *125*, 12810−12822.
(22) Kanagalingam, S.; Ngan, C. F.; Duhamel, J. *Macromolecules* **2002**, *35*, 8560−8570.
(23) Prazeres, T. J. V.; Beingessner, R.; Duhamel, J.; Olesen, K.; Shay, G.; Bassett, D. R. *Macromolecules* **2001**, *34*, 7876−7884.
(24) d'Agnillo, L.; Soares, J. B. P.; Penlidis, A. *J. Polym. Sci., Part B: Polym. Phys.* **2002**, *40*, 905−921.
(25) ASTM D 6474 *Annu. Book ASTM Stand.* **1999**, *08.03*.
(26) Lakowicz, J. R. *Principles of Fluorescence Spectroscopy*; Kluwer Academic/Plenum Publishers: New York, 1999: (a) pp 52−54; (b) p 9; (c) pp 368−388.
(27) Demas, J. N. *Excited-State Lifetime Measurements*; Academic Press: New York, 1983.
(28) Press, W. H.; Flannery, B. P.; Teukolsky, S. A.; Vetterling, W. T. *Numerical Recipes. The Art of Scientific Computing (Fortran Version)*; Cambridge University Press: Cambridge, England, 1992.
(29) Tachiya, M. *Chem. Phys. Lett.* **1975**, *33*, 289−292.
(30) Infelta, P. P.; Gratzel, M.; Thomas, J. K. *J. Phys. Chem.* **1974**, *78*, 190−195.
(31) Winnik, F. M. *Chem. Rev.* **1993**, *93*, 587−614.
(32) Mathew, A. K.; Duhamel, J.; Gao, J *Macromolecules* **2001**, *34*, 1454−1469.
(33) Berlman, I. B. *Handbook of fluorescence spectra of aromatic molecules.* Academic Press: New York, 1971: (a) p 330; (b) p 332.
(34) Demas, J. N.; Crosby, G. A. *J. Phys. Chem.* **1971**, *75*, 991−1024.
(35) Birks, J. B. *Photophysics of Aromatic Molecules*; Wiley: New York, 1970; p 351.
(36) Kramer, M. C.: Steger, J. R.; Hu, Y. X.; McCormick, C. L. *Macromolecules* **1996**, *29*, 1992−1997.
(37) Berlman, I. B. *Energy Transfer Parameters of Aromatic Compounds.* Academic Press: New York, 1973; p 312.

(38) Winnik, F. M. *Polymer* **1990**, *31*, 2125−2134.
(39) Malaika, S. A. *Reactive Modifiers for Polymers*, 1st ed.; Hu, G. H., Flat, J. J., Lambla, M., Eds.; Blackie Academic & Professional: London, 1997.
(40) Piçarra, S.; Gomes, P. T.; Martinho, J. M. G. *Macromolecules* **2000**, *33*, 3947−3950. Reynders, P.; Dreeskamp, H.; Kühnle, W.; Zachariasse, K. A. *J. Phys. Chem.* **1987**, *91*, 3982−3992.
(41) Bandrup, J.; Immergut, E. H.; Grulke, E. A. *Polymer Handbook*, 4th ed.; John Wiley & Sons: NY, 1999.
(42) Ito, K.; Guillet, J. E. *Macromolecules* **1979**, *12*, 1163−1167.
(43) Stryer, L.; Haugland, R. P. *Proc. Natl. Acad. Sci. U.S.A.* **1967**, *58*, 719−726.
(44) (a) Mizusaki, M.; Kopek, N.; Morishima, Y.; Winnik, F. M. *Langmuir* **1999**, *15*, 8090−8099. (b) Mizusaki, M.; Morishima, Y.; Winnik, F. M. *Macromolecules* **1999**, *32*, 4317−4326. (c) Yamazaki, A.; Song, J. M.; Winnik, F. M.; Brash, J. L. *Macromolecules* **1998**, *31*, 109−115. (d) Winnik, F. M.; Ottaviani, M. F.; Bossman, S. H.; Pan, W. S.; Garciagaribay, M.; Turro, N. J. *J. Phys. Chem.* **1993**, *97*, 12998−13005. (e) Ringsdorf, H.; Simon, J.; Winnik, F. M. *Macromolecules* **1992**, *25*, 7306−7312.
(45) (a) Smith, G. L.; McCormick, C. L. *Macromolecules* **2001**, *34*, 5579−5586. (b) Smith, G. L.; McCormick, C. L. *Macromolecules* **2001**, *34*, 918−924. (c) Hu, Y. X.; Smith, G. L.; Richardson, M. F.; McCormick, C. L. *Macromolecules* **1997**, *30*, 3526−3537.
(46) Anghel, D. F.; Alderson, V.; Winnik, F. M.; Mizusaki, M.; Morishima, Y. *Polymer* **1998**, *39*, 3035−3044.
(47) Sen, A.; Rubin, I. D. *Macromolecules* **1990**, *23*, 2519−2524.

MA035906E